

Design of Surface-Wave Band-Gaps for Planar Integrated Circuits Using Multiple Periodic Metallic Patch Arrays

Riccardo Leone and H.Y. David Yang

Department of Electrical Engineering and Computer Science
University of Illinois at Chicago

Abstract — In recent years, there has been significant interest in complete surface-wave elimination (meaning in all-possible directions) with the use of periodic elements in integrated circuit structures. This paper presents the theory for guided surface-wave and leaky-waves of multi-layer dielectric substrate with multiple planar periodic metallic patch arrays. This paper demonstrates that the use of multiple planar periodic patch arrays enlarges the surface-wave band-gap in all directions and provide more design flexibility as compared to a single planar periodic array. Several design examples are given. Design rules to obtain modeless (omnidirectional band-gap) substrates for integrated circuits are outlined.

I. INTRODUCTION

Recently, there has been significant interest in reducing or eliminating surface-wave in integrated circuit structures by using artificial periodic elements [1-4]. Printed circuit elements placed on a semiconductor substrate are known to generate surface-wave modes (or dielectric slab modes). There are two major effects of the surface-wave mode generation. Surface waves are considered losses in integrated circuits. Cross talk between devices printed monolithically on the surface of the substrate is mostly due to the surface wave interaction. It is often desirable to eliminate or minimize the surface wave effects. Recently, we had demonstrated both with theory and experiment that surface-wave are completely eliminated within a certain frequency-band by using a planar periodic array of patches on integrated circuit substrate [4]. The idea is to design patches at their resonances so that the slow-wave factor is large enough for the phase constant to meet the Bragg diffraction condition resulting band-gap (stop band) in all directions.

In this paper, we propose the use of multiple planar periodic patch arrays for surface-wave elimination. The idea is that in multi-layered structures with periodic metallic loading on each layer, we are able to design band-gaps due to each patch array and if the band-gaps are properly adjusted by choosing the patch dimensions, we will obtain wide controllable overall band-gap. In order to design the multi-layer band-gap, the modal analysis based on coupled integral equations and the method of moments is developed for two infinite patch

arrays. The analysis is validated with several limiting cases. Examples of the wide surface-wave band-gap design for two patch arrays are given. Of particular interest is the coupling effect of the two patch arrays on the modal diagram. Parametric study is performed to investigate the band-gap positions and widths as functions of the array element size and the layer material properties.

II. THEORY

The analysis of the problem is for wave propagation along a two-layer grounded dielectric slab with planar periodic patch arrays on each of the layer-interface as shown in Figure 1. The geometry is assumed planar. The pertinent problem is analyzed through an electric-field integral-equation formulation with unknown current on the periodic metallic elements. To simplify the analysis, it is assumed that the two patch arrays have the same array element spacing but with different element dimensions. As a result, the structure is periodic and Floquet's theorem can be applied to simplify the problem to the modeling of electromagnetic waves within a single cell. The Green's functions are obtained by solving the field solutions for horizontal sources in a two-layer planar structure. A Galerkin moment-method procedure is applied numerically to determine the current distributions on the patch element in the unit cell. Entire-domain basis functions based on patch cavity modes [4] are used to represent the current densities on the patches. The inner products of the resulting electric fields with a set of testing functions (the same entire-domain basis functions) are then set to zero in order to convert the electric field integral equation into the matrix equation. The matrix elements are in terms of a double infinite series and are evaluated numerically. A nontrivial solution for the current requires the matrix determinant to be zero, which results in a characteristic equation. The eigenvalues (propagation wavenumbers) are obtained from the roots of this equation for a given direction in the phase plane. Numerical results for the metallic patch structure are based on nine entire-domain basis functions for each current component.

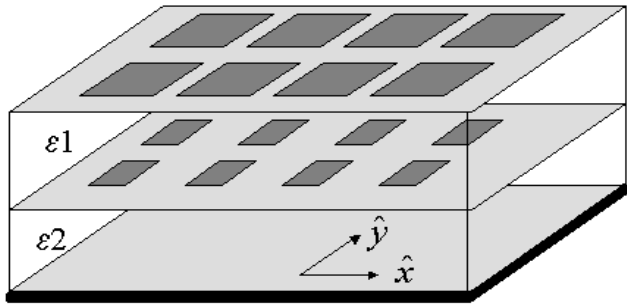


Figure 1. The geometry of a two-layer dielectric substrate with a planar array of patches residing on each layer interface.

III. RESULT DISCUSSION

The numerical results are validated for the limiting case of a single array with results available in [4]). It is done by setting the top layer thickness to zero so that the two patch arrays reside at the same layer interface. The two arrays with the same element sizes then become a new infinite patch array for one-layer substrate. Numerical results will be discussed first for a 100mil $\epsilon=10.2$ substrate, with array period 8x8 mm, and patch size 6x6 mm, where a spectral band-gap was found at (7.25-9.25) GHz by both theory and experiment [4]. A second array at the interface of two dielectric layers with patch size 4x4 mm, will be considered further as a case of study. Tables I and II refer to the case for the same thickness ($t_1=t_2=50\text{mil}$) of each layer.

(a). One patch array at a grounded dielectric ($\epsilon_1=\epsilon_2$) slab. As apparent from data shown in the diagonal of Table I, an effective way to position a spectral bandgap found in the structure under consideration is to decrease the substrate dielectric constant from 10.2 to 2.5. This allows one to design a band-gap at different frequencies by using different substrate materials.

(b). One patch array on top of a two-layered grounded dielectric slab. The availability of a second layer introduces more flexibility in the design by allowing the

control of the ratio between the two dielectric constants ϵ_1 and ϵ_2 , and thicknesses t_1 and t_2 . From table I (the case of 50mil thickness for each layer), it is seen that it is easier to produce surface-wave band-gaps by using a higher-dielectric constant layer close to the ground plane. The case suggests that lower dielectric materials correspond to higher band-gap frequencies. This is due to the fact that the band-gaps are due to the patch resonances that occur at higher frequencies for lower dielectric-constant materials.

(c). Two patch arrays stacked in a two-layered grounded dielectric slab. This case may be treated as a combination of two sub-cases, one of which being the case (b) and the other one as the case (a) but with a dielectric cover. It is found, by comparing the corresponding dispersion diagrams, that the propagation characteristics for the case (c) are very similar to the first sub-case (namely, only the top patch array) as long as $\epsilon_1 \approx \epsilon_2$ or $\epsilon_1 > \epsilon_2$, as apparent from the two tables in terms of band-gap similarity. It implies that we may consider the insertion of the second array as a perturbation (if any) of the propagation characteristics. On the other hand, when $\epsilon_1 \leq 5.4$ and $\epsilon_2=10.2$, the modes within the structure are dictated by the bottom patch array. Again, this observation can be explained by the patch resonances as when the lower layer has much higher dielectric constant, the patch characteristics are mostly determined by the cavity it forms with the ground plane. As a result, the upper layer patch array has insignificant effect on the band-gap as observed from the first column of Table II. However by comparing the end of the first row of Tables I and II, it is observed that with the second array results in a larger spectral band-gap (9-10 GHz instead of 9.5-10 GHz), when $\epsilon_1=10.2$, and $\epsilon_2=2.5$. Similar observation is found for $\epsilon_2=10.2$, and $\epsilon_1=2.5$ (the last cell in the first column of Table II), where the band-gap is at (10-10.7) GHz and the case for without the top patch arrays is (10.5 - 10.8) GHz. The larger band-gap due to the presence of a second array found in both cases is essentially due to mutual coupling of the two patch arrays.

TABLE I
Omnidirectional Band-Gaps for case (a) and (b) (accuracy within 0.175GHz)

$\epsilon=(\epsilon_1, \epsilon_2)$	10.2	7.2	5.4	4.0	2.5
10.2	7.25 – 9.25	8.25 – 9.4	8.5 – 9.5		9.5 – 10
7.2	8.5 – 10	9 – 10.8	9.45 – 11.1		
5.4	9.4 – 11	9.8 – 11.5	10.5 – 12.1		
4.0	10.3 – 11.8			11.8 – 13.4	13.4 – 14.2
2.5	12.1 – 12.9		13.1 – 14	13.8 – 14.5	14.75 – 15.6

TABLE II
Omnidirectional Band-Gaps for case (c) (accuracy within 0.175GHz)

$\epsilon = (\epsilon_1, \epsilon_2)$	10.2	7.2	5.4	4.0	2.5
10.2	8 – 9	8.1 – 9.5	8 – 9.5		9 – 10
7.2	8.25 – 10	9 – 10.8	9.4 – 11.3		
5.4	8.9 – 10.1	9.75 – 11.3	10.5 – 12.1		
4.0	9.4 – 10.8				
2.5	10 – 10.7	11.2 – 12.25	12.25 – 13.4	13.3 – 14.3	14.8 – 15.5

The use of two patch arrays may not always result in band-gap enlargement. It is possible that the opposite is true. It is also possible that the presence of the second array may completely destroy a spectral BG, as is found in the case of 25+25mil substrate, with $\epsilon = (2.5, 10.2)$. It is also possible that the use of two patch arrays introduces additional band-gap. Typical examples of dispersion diagram are shown in Figures 2-5 for two cases. Note that the 0-degree (\hat{x}) and 45 degree ($\hat{x} + \hat{y}$) propagation modes are mostly distinct for a square array. The band-gap in both directions usually implies that the band-gap is omnidirectional. The mode diagrams are $\beta / k_o - f$ diagrams. Figures 2-3 and Figures 4-5 are also for the case in the last and the third cell of the first column in Table II, respectively. These Figures are for the case where the top-layer dielectric constant is 2.5 and 5.4, respectively and other parameters are the same. It is seen that the higher the top-layer dielectric constant, the lower the band-gap frequencies. Figures 6 and 7 demonstrate the existence of omni-directional bandgaps through the photonic band structures.

REFERENCES

- [1] H.Y.D. Yang, "Characteristics of guided and leaky waves on a thin-film structure with planar material gratings," *IEEE Trans. Microwave Theory and Tech.*, vol. MTT-45, no. 3, pp. 428-435, Mar. 1997.
- [2] D. Sievenpiper, L. Zhang, R.F. Broas, N.G. Alexopoulos, and E. Yablonovitch, "High-impedance electromagnetic surfaces with a forbidden frequency band," *IEEE Trans. Microwave Theory and Tech.*, vol. MTT-47, no. 11, pp. 2059-2074, Nov. 1999.
- [3] R. Coccioni, F.R. Yang, K.P. Ma, and T. Itoh, "Aperture-coupled patch antenna on a UC-PBG substrate," *IEEE Trans. Microwave Theory and Tech.*, vol. MTT-47, no. 11, pp. 2123-2130, Nov. 1999.
- [4] H.Y.D. Yang, R. Kim, D.R. Jackson, "Design considerations for modeless integrated circuit substrates using planar periodic patches," *IEEE Trans. Microwave Theory and Tech.*, vol. MTT-48, no. 12, pp. 2233-2239, Dec. 2000.

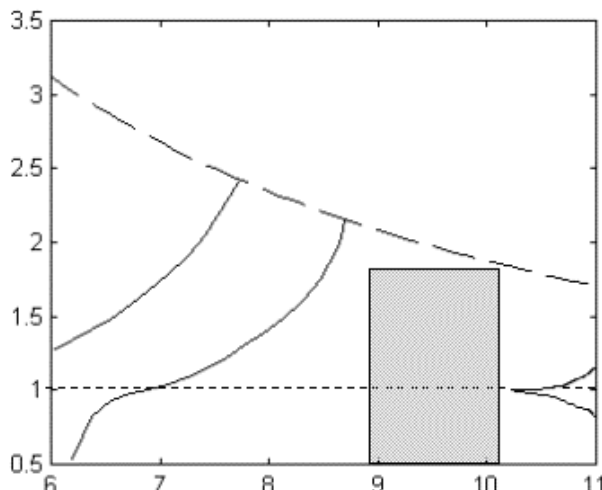


Fig. 2: Normalized phase constant (β/K_o) vs frequency propagation in $\phi=0$ direction (table II, 1st col., 3rd cell)

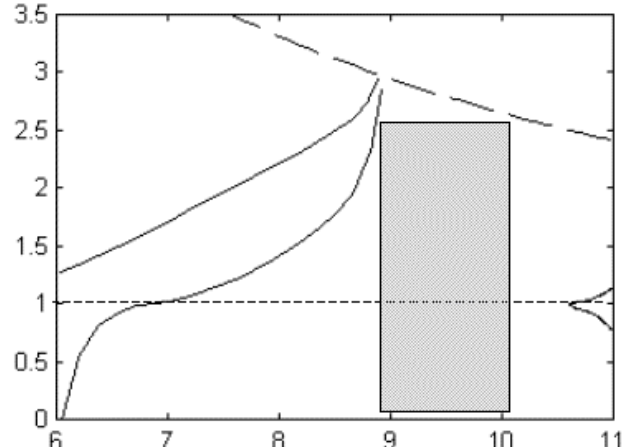


Fig. 3: Normalized phase constant (β/K_o) vs freq. for propagation in $\phi=45$ direction (table II, 1st col., 3rd cell)

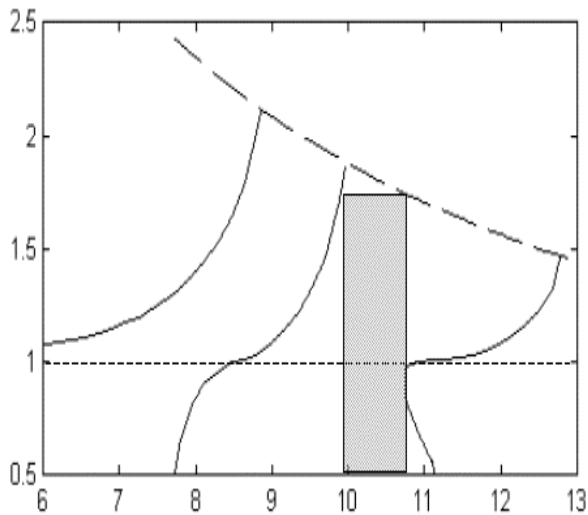


Fig. 4: Normalized phase constant (β/K_0) vs freq. for propagation in $\phi=0$ direction (table II, 1st col., last cell)

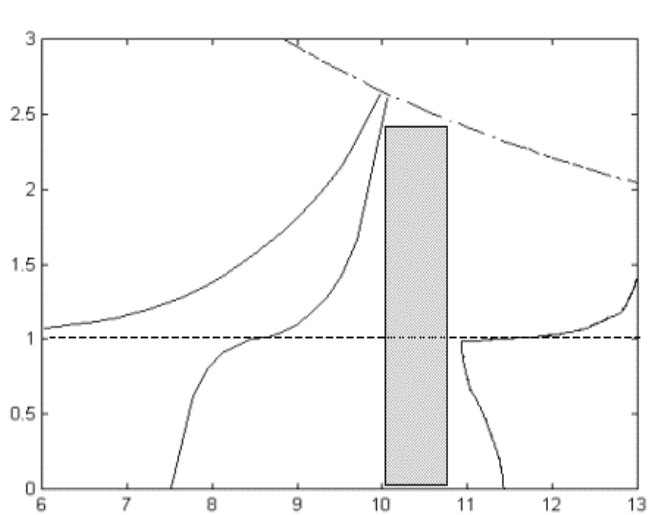


Fig. 5: Normalized phase constant (β/K_0) vs freq. for propagation in $\phi=45$ direction (table II, 1st col., last cell)

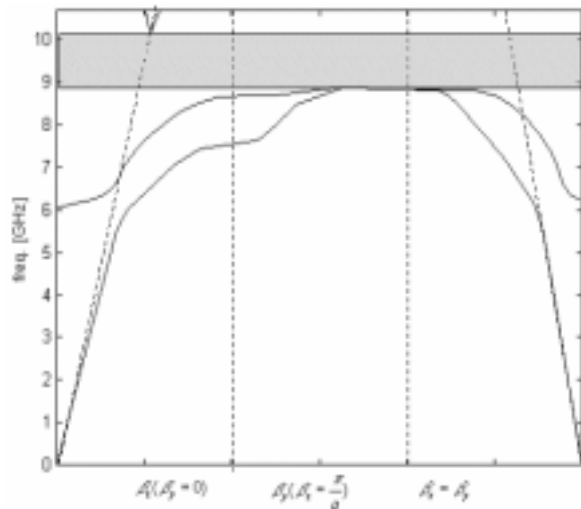


Fig. 6: Mode band diagram for the case corresponding to table II, 1st col., 3rd cell. The strip in gray encloses an omnidirectional bandgap.

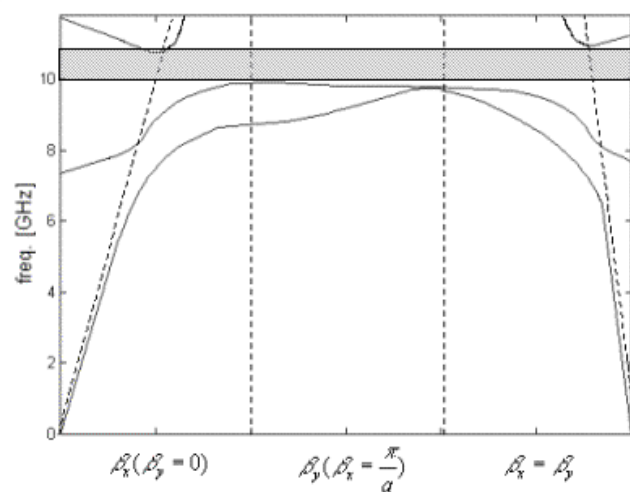


Fig. 7: Mode band diagram for the case corresponding to table II, 1st col., last cell. The strip in gray encloses an omnidirectional bandgap.